Mineralogical Magazine (2024), **88**, 218–227
doi:10.1180/mgm.2024.14

Article

Crystal structure of Pb-bearing watanabeite from Pefka, Greece

Cristian Biagioni[1,2], Panagiotis Voudouris[3], Yves Moëlo[4], Jiří Sejkora[5], Zdeněk Dolníček[5], Silvia Musetti[1] and Daniela Mauro[1,6]

[1]Dipartimento di Scienze della Terra, Università di Pisa, Via Santa Maria, 53, I-56126 Pisa, Italy; [2]Centro per l'Integrazione della Strumentazione Scientifica dell'Università di Pisa, Università di Pisa, Italy; [3]Faculty of Geology and Geoenvironment, National and Kapodistrian University of Athens, 15784 Athens, Greece; [4]Université de Nantes, CNRS, Institut des Matériaux Jean Rouxel, IMN, F-44000 Nantes, France; [5]Department of Mineralogy and Petrology, National Museum, Cirkusová 1740, 193 00, Prague 9, Czech Republic; and [6]Museo di Storia Naturale, Università di Pisa, Via Roma 79, I-56011 Calci (PI), Italy

Abstract

Watanabeite from the Pefka epithermal deposit, northeastern Greece, was examined using single-crystal X-ray diffraction and electron microprobe analysis. The empirical formula of watanabeite is $Cu_{3.93}Fe_{0.10}Ag_{0.01}Pb_{0.23}As_{1.55}Sb_{0.19}S_{4.99}$. This mineral is orthorhombic, space group *Amm*2, with unit-cell parameters $a = 10.9601(5)$, $b = 14.6498(8)$, $c = 10.3001(5)$ Å, $V = 1653.82(14)$ Å^3 and $Z = 8$. The crystal structure was solved and refined to $R_1 = 0.0471$ for 2108 unique reflections with $F_o > 4\sigma(F_o)$ and 123 refined parameters. The crystal structure of watanabeite can be described as a three-dimensional framework of Cu-centred tetrahedra; cavities of the tetrahedral scaffolding host Cu_6S and $As_2(Pb,Sb,As)_2S_7$ clusters. On the basis of structural data, the formula of watanabeite could be written as $^{[III]}Cu_3{}^{[IV]}Cu_5As_3(Pb,Sb,As)S_{10}$ ($Z = 4$), considering the three independent three-fold Cu sites and the three independent tetrahedrally coordinated Cu sites as aggregated positions. The occurrence of Pb^{2+} in watanabeite is probably related to the substitution $Cu^+ + (As,Sb)^{3+} = 2Me^{2+}$, where Me = Pb, Fe, Zn and formally divalent Cu. The relationships with tetrahedrite-group minerals are discussed on the basis of the refined structural model, highlighting possible crystal chemical implications of such relationships.

Keywords: watanabeite; sulfosalt; copper; arsenic; lead; crystal structure; Pefka; Greece

(Received 3 December 2023; accepted 23 February 2024; Accepted Manuscript published online: 4 March 2024; Associate Editor: František Laufek)

Introduction

Watanabeite, ideally $Cu_4As_2S_5$, was described by Shimizu *et al.* (1993) from the Teine mine, Sapporo, Hokkaido, Japan, in association with emplectite, native bismuth, and members of the tennantite–tetrahedrite series. The empirical formula of type material is $(Cu_{3.94}Mn_{0.03}Ag_{0.01})_{\Sigma 3.98}(As_{1.25}Sb_{0.72}Bi_{0.07})_{\Sigma 2.04}S_{4.98}$; some variations in the As/(As+Sb) ratio were reported by Shimizu *et al.* (1993), who also found a hypothetical Sb-analogue from the Takinosawa deposit. Owing to the small grain size, single-crystal X-ray diffraction data were not collected and the identification was based on the powder X-ray diffraction pattern only, similar but not identical to that of tetrahedrite-group minerals. Shimizu *et al.* (1993) proposed an orthorhombic cell, with $a = 14.51(1)$, $b = 13.30(1)$, $c = 17.96(1)$ Å and $Z = 16$.

Later, watanabeite was reported by Paar *et al.* (2002), Makovicky *et al.* (2005) and Márquez-Zavalía and Galliski (2007) from Catamarca, Argentina, with variable replacement of As by Sb and Bi and the substitution of Cu by Zn, Fe, and minor Mn and Ag. Other occurrences are known from Greece, where Voudouris *et al.* (2005, 2011) and Repstock *et al.* (2015) reported the presence of watanabeite from the Perama Hill, St. Philippos, and Pefka deposits. Zheng *et al.* (2021) gave chemical data for watanabeite from the Jiama porphyry system, south Tibet. Some other occurrences should deserve further investigations: for instance, Sidorov *et al.* (2020) reported a potential Sb-analogue of watanabeite from the Maletoyvayam deposit, Koryak Highland, Russia, and the same species may occur at the Pefka deposit (Repstock *et al.*, 2015). Finally, watanabeite is cited also from other localities but no chemical or structural data are given to confirm such an identification (e.g. Papavasiliou *et al.*, 2016; Ahmed *et al.*, 2018; Efremov *et al.*, 2021). As will be shown later, some of these identifications of watanabeite reported in literature probably correspond to other mineral species.

During the investigation of tetrahedrite-group minerals from the Pefka deposit, leading to the identification of tennantite-(In) (Voudouris *et al.*, 2023), Pb-bearing watanabeite was identified and a grain suitable for single-crystal X-ray diffraction (XRD) study was found. In this paper the description of the crystal structure of watanabeite is reported, along with a discussion of its crystal chemistry.

Experimental

The specimen studied is represented by the type material of tennantite-(In), kept in the mineralogical collection of the

Corresponding author: Cristian Biagioni; Email: cristian.biagioni@unipi.it

Cite this article: Biagioni C., Voudouris P., Moëlo Y., Sejkora J., Dolníček Z., Musetti S. and Mauro D. (2024) Crystal structure of Pb-bearing watanabeite from Pefka, Greece. *Mineralogical Magazine* **88**, 218–227. https://doi.org/10.1180/mgm.2024.14

Museo di Storia Naturale of the Università di Pisa (Italy), under catalogue number 20029. Watanabeite occurs as anhedral grains, up to 0.2 mm in size, associated with tennantite-(Fe), tennantite-(In), roquesite, galena, bournonite and seligmannite in a quartz gangue (Fig. 1).

The quantitative chemical analysis of watanabeite was carried out using a Cameca SX 100 electron microprobe (National Museum of Prague, Czech Republic) and the following analytical conditions: wavelength dispersive spectroscopy mode, accelerating voltage 20 kV, beam current 20 nA, beam diameter 0.7 µm. Standards (element, emission line) were: Ag (Ag*L*α), CdTe (Cd*L*α), chalcopyrite (Cu*K*α, S*K*α), InAs (In*L*α), Mn (Mn*K*α), NiAs (As*L*β), PbS (Pb*M*α), PbSe (Se*L*β), PbTe (Te*L*α), pyrite (Fe*K*α), Sb_2S_3 (Sb*L*α) and ZnS (Zn*K*α). Contents of other elements including Au, Bi, Co, Ga, Ge, Hg, Ni, Sn and Tl were always below detection limits. Matrix correction by the *PAP* algorithm (Pouchou and Pichoir, 1985) was applied to the data. Results are reported in Table 1.

Single-crystal XRD intensity data of watanabeite were collected using a Bruker D8 Venture diffractometer (50 kV and 1.4 mA) equipped with an air-cooled Photon III detector, and microfocus Mo*K*α radiation (C.I.S.U.P., University of Pisa, Italy). The detector-to-crystal distance was set to 38 mm. Intensity data were collected using φ and ω scan modes, in 0.5° slices, with an exposure time of 15 s per frame. A total of 2072 frames was collected. Frames were integrated with the Bruker *SAINT* software package using a narrow-frame algorithm. The integration of the data using an *A*-centred orthorhombic unit cell yielded a total of 24,223 reflections to a maximum θ angle of 28.34°. The final cell constants are based upon the refinement of the XYZ-centroids of 8598 reflections above $20\sigma I$, with $4.834° < 2\theta < 55.15°$. The refined unit-cell parameters are $a = 10.9601(5)$, $b = 14.6498(8)$, $c = 10.3001(5)$ Å and $V = 1653.82(14)$ Å^3. Data were then corrected for Lorentz-polarisation, absorption and background. The statistical tests on the distribution of $|E|$ values ($|E^2 - 1| = 0.912$) suggested the possible centric nature of watanabeite. However, the solution of its crystal structure in the space group *Ammm* was unsuccessful. Eventually, the crystal structure was solved using *ShelxTL* and refined through *Shelxl-2018* (Sheldrick, 2015) in the space group *Amm*2. Neutral scattering curves were taken from the *International Tables for Crystallography* (Wilson, 1992). In the crystal structure of watanabeite from the Pefka deposit, ten cation and eight S sites were located. Among cation positions, six are fully occupied by Cu, three by As, and one is a mixed and split *M*(1) site hosting As, Sb and Pb. The displacement parameters of these two split sub-positions were constrained to be the same. The location of minor Fe and Ag was not identified. A racemic twin was modelled, resulting in the ratio 0.13/0.87 between the two components, thus supporting the acentric nature of watanabeite. After several cycles of anisotropic refinement, the R_1 factor converged to 0.0471 for 2108 unique reflections with $F_o > 4\sigma(F_o)$ and 123 refined parameters. Some relatively high (unmodelled) residuals (up to ~ 4 e^-/Å^3) were observed in the difference-Fourier map. The three main maxima are located around Cu atoms hosted at the Cu(4), Cu(6) and Cu(1) sites. These maxima may be related to an incomplete modelling for the racemic twin. Moreover, Cu atoms at the Cu(4) and Cu(6) sites have a bonding environment similar to that of atoms hosted at the *M*(2) site in tetrahedrite-group minerals, which can be split owing to positional disorder (e.g. Biagioni *et al.*, 2020a); it cannot be excluded that a similar phenomenon may occur in watanabeite. The residual around the split *M*(1) site is probably due to the incomplete modelling of the anisotropic displacement parameters of the As [*M*(1a)] and Pb [*M*(1b)] positions, as these values at both sub-positions were constrained to be the same. Finally, reconstructed precession images of the reciprocal lattice of watanabeite revealed the occurrence of some misoriented grains in the sample studied, possibly being an additional reason for the presence of some residuals in the difference-Fourier map.

Table 1. Chemical data for watanabeite (wt.%) and atoms per formula unit (apfu) on the basis of 11 apfu.

Element	wt.%	range (n = 69)	e.s.d.	apfu	range	e.s.d.
Cu	41.57	40.53–42.91	0.51	3.932	3.852–4.005	0.039
Ag	0.26	0.12–0.35	0.05	0.014	0.007–0.020	0.003
Mn	0.01	0.00–0.13	0.03	0.001	0.000–0.014	0.003
Fe	0.91	0.18–2.37	0.50	0.097	0.020–0.252	0.053
Zn	0.02	0.00–0.23	0.05	0.002	0.000–0.021	0.005
Cd	0.01	0.00–0.13	0.03	0.000	0.000–0.007	0.002
Pb	7.83	6.06–8.64	0.60	0.227	0.174–0.249	0.018
As	19.32	18.16–20.28	0.42	1.550	1.483–1.628	0.029
In	0.02	0.00–0.06	0.02	0.002	0.000–0.021	0.005
Sb	3.78	2.38–5.59	0.69	0.187	0.117–0.279	0.035
S	26.60	26.23–26.98	0.20	4.986	4.940–5.045	0.023
Se	0.03	0.00–0.20	0.05	0.002	0.000–0.015	0.004
Te	0.02	0.00–0.13	0.04	0.001	0.000–0.006	0.002
Total	100.36	99.57–101.11	0.34			

n = number of spot analyses; e.s.d. = estimated standard deviation.

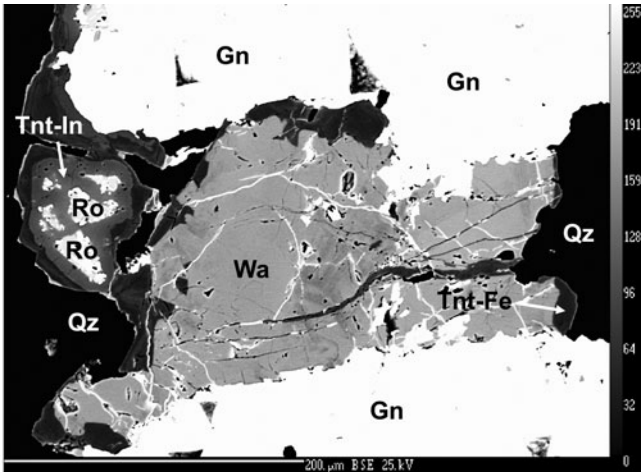

Figure 1. Back-scattered electron image of watanabeite from the Pefka deposit, Greece. Mineral symbols (after Warr, 2021): Gn = galena; Qz = quartz; Ro = roquesite; Tnt-Fe = tennantite-(Fe); Tnt-In = tennantite-(In); Wa = watanabeite. Catalogue number 20029, Museo di Storia Naturale, Università di Pisa, Italy.

Details of data collection and refinement for watanabeite are given in Table 2, whereas fractional atomic coordinates and displacement parameters, as well as selected bond distances, are given in Tables 3 and 4. Table 5 reports the bond-valence sums, calculated using the bond parameters of Brese and O'Keeffe (1991). The crystallographic information file (cif) has been deposited with the Principal Editor of *Mineralogical Magazine* and is available as Supplementary material (see below).

Table 2. Summary of crystal data and parameters describing data collection and refinement for watanabeite.

Crystal data	
X-ray formula	$Cu_4Pb_{0.26}As_{1.74}S_5$
Crystal size (mm)	0.090 × 0.070 × 0.050
Space group	*Amm*2
a (Å)	10.9601(5)
b (Å)	14.6498(8)
c (Å)	10.3001(5)
V ($Å^3$)	1653.82(14)
Z	8
Data collection and refinement	
Radiation, wavelength (Å)	Mo*K*α, λ = 0.71073
Temperature (K)	293(2)
$2\theta_{max}$ (°)	56.67
Measured reflections	24,223
Unique reflections	2225
Reflections with $F_o > 4\sigma(F_o)$	2108
R_{int}	0.0582
$R\sigma$	0.0383
Range of *h*, *k*, *l*	$-14 \le h \le 14$ $-19 \le k \le 18$ $-13 \le l \le 13$
R_1 $[F_o > 4\sigma(F_o)]$	0.0471
R_1 (all data)	0.0500
wR_2 (on F_o^2)[1]	0.1113
Goof	1.138
Absolute structure parameter[2]	0.131(19)
Number of least-squares parameters	123
Maximum and minimum residual peak ($e^- Å^{-3}$)	+4.14 [at 0.45 Å from Cu(4)] −1.51 [at 0.57 Å from Cu(4)]

[1] $w = 1/[\sigma^2(F_o^2) + (0.0472P)^2 + 38.2973P]$.

[2] Flack (1983)

Results and discussion

Chemical formula of watanabeite

The chemical formula of watanabeite from the Pefka epithermal deposit, calculated on the basis of 11 atoms per formula unit (apfu), neglecting minor Mn, Zn, Cd, In, Se and Te, is $Cu_{3.93}Fe_{0.10}Ag_{0.01}Pb_{0.23}As_{1.55}Sb_{0.19}S_{4.99}$.

The examination of available literature data, coupled with the results of new electron microprobe analyses performed during this study, allows discussion of two points: (1) distinction of watanabeite from tetrahedrite-group minerals; and (2) chemical features of watanabeite.

Chemical distinction of watanabeite from tetrahedrite-group minerals

Watanabeite shows the same chemical constituents as tennantite-(Cu) (Biagioni *et al.*, 2022b), i.e. Cu, As and S, and similar (Cu+As)/S ratios, i.e. 1.200 and 1.231, respectively. On the contrary, the ratio between Cu and As is very different, being 2 in watanabeite and 3 in tennantite-(Cu). An examination of the available literature shows that Cu can be replaced by Zn, Fe and other minor elements (e.g. Mn or Ag), whereas As can be substituted by Sb, Bi and Pb.

All the available chemical data referred to as watanabeite in Fig. 2 is plotted as a function of the Cu*/As* *vs.* *Me**/S ratios, where: Cu* is the sum of all metals (Cu+Ag+Zn+Fe… without Pb); As* is the sum of all semi-metals (with Pb); and *Me** is the sum of all metals (including Cu) and semimetals. It is apparent that not all the samples labelled as watanabeite on the basis of chemical analysis only are correctly identified as follows. (1) Watanabeite from Cerro Atajo and Mina Capillitas, Catamarca, Argentina, described by Márquez-Zavalía and Galliski (2007), is actually tennantite-(Zn); on the contrary, the two analyses reported by Paar *et al.* (2002) and Makovicky *et al.* (2005) from Cerro Atajo correspond to watanabeite. (2) Chemical analyses of watanabeite from Pefka reported by Repstock *et al.* (2015) correspond to watanabeite (analyses 2–6), whereas analyses 7–13 can be identified as tennantite-(Fe) and tetrahedrite-(Fe). Analysis 1 is probably watanabeite with an admixture of a minor amount of a tetrahedrite-group mineral. (3) Two spot analyses reported by Voudouris *et al.* (2005) from St. Philippos have low Cu*/As* ratios; however, the authors stated that watanabeite was included in galena and the high Pb content could be interpreted as due to the occurrence of inclusions of this lead sulfide. (4) The potential Sb-analogue of watanabeite described from the Maletoyvayam deposit by Sidorov *et al.* (2020) has a Cu*/As* ratio similar of those of tetrahedrite-group minerals, but with a lower *Me**/S ratio, close to 1. This could be an (As,Se)-rich famatinite.

This review of available chemical data is a fundamental step for discussing the chemical features of 'true' watanabeite.

Table 3. Sites, Wyckoff positions, site occupancy, fractional atomic coordinates and equivalent isotropic displacement parameters ($Å^2$) for watanabeite.

Site	Wyckoff position	Site occupancy	*x*/*a*	*y*/*b*	*z*/*c*	U_{eq}
Cu(1)	8*f*	$Cu_{1.00}$	0.33141(14)	0.25882(11)	0.69658(19)	0.0218(4)
Cu(2)	8*f*	$Cu_{1.00}$	−0.15897(16)	0.37333(11)	−0.06921(19)	0.0218(4)
Cu(3)	4*e*	$Cu_{1.00}$	½	0.12479(18)	0.9574(3)	0.0259(6)
Cu(4)	8*f*	$Cu_{1.00}$	0.1368(3)	0.38465(19)	0.4520(3)	0.0571(9)
Cu(5)	2*a*	$Cu_{1.00}$	0	½	0.2184(6)	0.0622(18)
Cu(6)	2*a*	$Cu_{1.00}$	0	½	0.6551(4)	0.0417(12)
M(1a)	4*c*	$As_{0.481(8)}$	0.3128(9)	0	0.6962(10)	0.0282(7)
M(1b)	4*c*	$Pb_{0.519(8)}$	0.2787(3)	0	0.7205(3)	0.0282(7)
As(1)	4*c*	$As_{1.00}$	0.33662(15)	½	0.7008(2)	0.0141(4)
As(2)	4*d*	$As_{1.00}$	0	0.24455(13)	0.17901(17)	0.0130(4)
As(3)	4*e*	$As_{1.00}$	½	0.38917(13)	0.9266(2)	0.0194(4)
S(1)	4*d*	$S_{1.00}$	0	0.3827(3)	0.0799(4)	0.0171(9)
S(2)	4*e*	$S_{1.00}$	½	0.2541(3)	0.8286(4)	0.0137(8)
S(3)	8*f*	$S_{1.00}$	0.1555(3)	0.2640(2)	0.3188(3)	0.0143(6)
S(4)	4*c*	$S_{1.00}$	0.1540(4)	½	0.7987(4)	0.0134(8)
S(5)	8*f*	$S_{1.00}$	0.3140(3)	0.3825(2)	0.5621(3)	0.0152(6)
S(6)	2*b*	$S_{1.00}$	½	0	0.8140(7)	0.0215(14)
S(7)	8*f*	$S_{1.00}$	0.6648(3)	0.3670(2)	0.0595(3)	0.0168(6)
S(8)	2*a*	$S_{1.00}$	0	½	0.4374(7)	0.0217(12)

Table 4. Selected bond distances (in Å) for watanabeite.

Cu(1)–S(5)	2.289(4)	Cu(2)–S(4)	2.302(3)	As(1)–S(8)	3.784(5)	As(2)–S(3)	2.249(3)	*M*(1a)–S(6)	2.384(10)
Cu(1)–S(2)	2.295(3)	Cu(2)–S(3)	2.319(4)	As(1)–S(1)	3.792(4)	As(2)–S(3)	2.249(3)	*M*(1a)–S(7)	2.417(7)
Cu(1)–S(7)	2.322(4)	Cu(2)–S(1)	2.327(3)	As(1)–S(1)	3.792(4)	As(2)–S(1)	2.267(5)	*M*(1a)–S(7)	2.417(7)
Cu(1)–S(3)	2.327(3)	Cu(2)–S(7)	2.345(4)	<As(1)–S>	3.207	<As(2)–S>	2.255	<*M*(1a)–S>	2.406
<Cu(1)–S>	2.308	<Cu(2)–S>	2.323						
				As(1)–S(4)	2.242(5)	As(3)–S(2)	2.221(5)	*M*(1a)–*M*(1b)	0.450(9)
Cu(3)–S(5)	2.309(4)	Cu(4)–S(3)	2.248(4)	As(1)–S(5)	2.250(3)	As(3)–S(7)	2.289(3)		
Cu(3)–S(5)	2.309(4)	Cu(4)–S(5)	2.249(4)	As(1)–S(5)	2.250(3)	As(3)–S(7)	2.289(3)	*M*(1b)–S(6)	2.610(4)
Cu(3)–S(2)	2.313(5)	Cu(4)–S(8)	2.264(3)	<As(1)–S>	2.247	<As(3)–S>	2.266	*M*(1b)–S(7)	2.633(4)
Cu(3)–S(6)	2.350(5)	<Cu(4)–S>	2.254					*M*(1b)–S(7)	2.633(4)
<Cu(3)–S>	2.320							<*M*(1b)–S>	2.625
		Cu(6)–S(8)	2.243(8)						
Cu(5)–S(1)	2.233(6)	Cu(6)–S(4)	2.243(5)						
Cu(5)–S(1)	2.233(6)	Cu(6)–S(4)	2.244(5)						
Cu(5)–S(8)	2.256(9)	<Cu(6)–S>	2.243						
<Cu(5)–S>	2.241								

Table 5. Weighted bond-valence sums (in valence units) for watanabeite.

Site	S(1)	S(2)	S(3)	S(4)	S(5)	S(6)	S(7)	S(8)	Σcations	Theoretical
Cu(1)		$0.31^{\downarrow\times2}$	0.28		0.31		0.29		1.19	1.00
Cu(2)	$0.28^{\downarrow\times2}$		0.29	$0.30^{\downarrow\times2}$			0.27		1.14	1.00
Cu(3)		0.29			${}^{2\times\rightarrow}0.30$	$0.27^{\downarrow\times2}$			1.16	1.00
Cu(4)			0.35		0.35			$0.34^{\downarrow\times4}$	1.04	1.00
Cu(5)	${}^{2\times\rightarrow}0.37$							0.34	1.08	1.00
Cu(6)				${}^{2\times\rightarrow}0.35$				0.36	1.06	1.00
M(1a)						$0.36^{\downarrow\times2}$	${}^{2\times\rightarrow}0.33$		1.02	
M(1b)	${}^{2\times\rightarrow}0.02^{\downarrow\times2}$					$0.51^{\downarrow\times2}$	${}^{2\times\rightarrow}0.48$	0.02	1.53	
As1				1.05	${}^{2\times\rightarrow}1.03$				3.11	3.00
As2	0.98		${}^{2\times\rightarrow}1.03$						3.04	3.00
As3		1.11					${}^{2\times\rightarrow}0.92$		2.95	3.00
Σanions	1.95	2.02	1.95	2.00	1.99	2.28	2.29	2.08		
Theoretical	2.00	2.00	2.00	2.00	2.00	2.00	2.00	2.00		

Note: left and right superscripts indicate the number of equivalent bonds involving cations and anions, respectively. The following site occupancies were used for *M*(1a) and *M*(1b) sites, respectively: *M*(1a) = $Sb_{0.21}As_{0.15}$; *M*(1b) = $Pb_{0.47}Sb_{0.17}$.

Chemical features of watanabeite

Scrutiny of the available data allows us to report the following chemical features for watanabeite:

(1) Cu content is usually close to 4 apfu, ranging between 3.53 and 4.20 apfu. The lowest value was reported in a sample from St. Philippos, Greece (Voudouris *et al.*, 2005), characterised by the highest Ag content so far reported in watanabeite.

(2) Silver content is usually low (<0.02 apfu). Only watanabeite from St. Philippos, Greece (Voudouris *et al.*, 2005), has up to 0.22 Ag apfu.

(3) Minor metals which can be present in watanabeite are Fe and Zn (up to 0.40 and 0.10 apfu, respectively, in a sample from the Perama Hill, Greece – Voudouris *et al.*, 2011). Up to

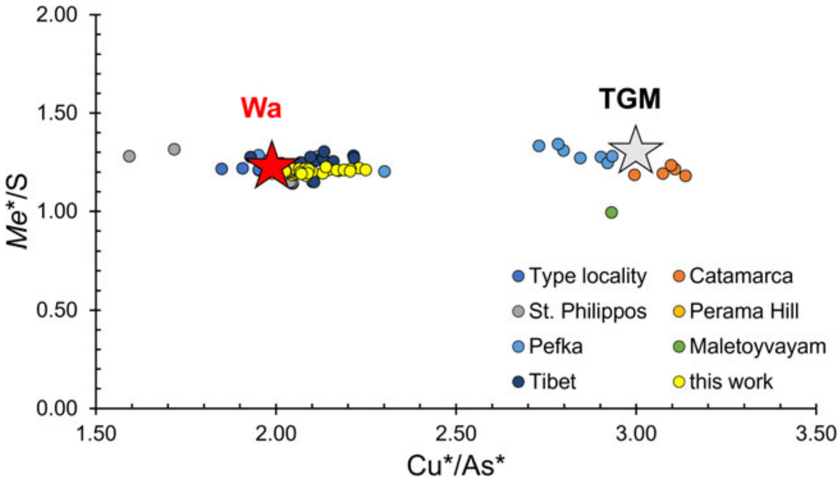

Figure 2. Diagram showing the relation between Cu*/As* *vs.* Me*/S ratios for samples of watanabeite described in literature. Red and grey stars indicate the ideal values for watanabeite (Wa) and tetrahedrite-group minerals (TGM). Chemical data are after Shimizu *et al.* (1993) for the type locality; Paar *et al.* (2002), Makovicky *et al.* (2005), and Márquez-Zavalía and Galliski (2007) for Catamarca province, Argentina; Voudouris *et al.* (2005) for St. Philippos, Greece; Voudouris *et al.* (2011) for Perama Hill, Greece; Repstock *et al.* (2015) for Pefka, Greece; Sidorov *et al.* (2020) for Maletoyvayam, Russia; Zheng *et al.* (2021) for the Jiama porphyry system, South Tibet. Yellow circles represent analytical data from our study.

0.40 apfu of Pb have been measured in samples of Ag-bearing watanabeite from the St. Philippos deposit (Voudouris *et al.*, 2005); as this sample was admixed with galena, it cannot be excluded that some Pb is due to the occurrence of inclusions of this lead sulfide. Minor amounts of Mn (up to 0.07 apfu in type material from Japan – Shimizu *et al.*, 1993) and Hg (up to 0.03 apfu in samples from the Jiama porphyry system, Tibet – Zheng *et al.*, 2021) are also reported;

(4) Arsenic content is variable, ranging between 1.01 and 1.98 apfu. In the Introduction it was reported that a possible existence of the Sb-analogue of watanabeite was proposed by Shimizu *et al.* (1993) who reported the identification of a sample from the Takinosawa deposit, Japan, having an As-to-Sb ratio of 41:59; other occurrences of possible Sb-analogues of watanabeite (e.g. Repstock *et al.*, 2015; Sidorov *et al.*, 2020) correspond to members of the tetrahedrite group or to famatinite. The highest amount of Sb so far observed is 0.88 apfu in watanabeite from the Jiama porphyry system, South Tibet (Zheng *et al.*, 2021). Similar values were reported by Shimizu *et al.* (1993), up to 0.87 apfu.

(5) Bismuth is reported in watanabeite, up to 0.44 apfu in samples from Cerro Atajo, Argentina (Makovicky *et al.*, 2005).

(6) The occurrence of minor Sn (up to 0.05 apfu) is known from Perama Hill, Greece (Voudouris *et al.*, 2011). Its crystal-chemical role is unknown as Sn can occur as Sn^{2+} or Sn^{4+}.

(7) Sulfur is usually the only anion occurring in watanabeite. Selenium and Te are reported, usually in very low amounts (up to 0.04 and 0.03 apfu, respectively). Finally, the role of Te is ambiguous, as it could also act as a cation (Te^{4+}) as observed in tetrahedrite-group minerals (e.g. Biagioni *et al.*, 2020a).

Repstock *et al.* (2015) observed that whereas the sum of metals (e.g. Cu, Ag, Hg, Fe) can be above 4 apfu, the sum of As, Sb and Bi can be below 2 apfu; on this basis, they speculated that Fe^{3+} may occur in watanabeite, as a substituent for As, Sb and Bi. Actually, the Fe-rich watanabeite they described is a member of the tetrahedrite-(Fe)/tennantite-(Fe) series, and the amount of Fe in true watanabeite is small. However, the excess of Cu, Ag and other metals (up to 0.32 apfu) and the deficit of metalloids (down to 1.70 apfu) was observed in watanabeite from other occurrences. The sum (Cu + Ag) is not clearly correlated with other metals *Me* (Fig. 3a), whereas the content of As + Sb + Bi is related to the ratio between Cu and the sum (Cu + *Me*) (this ratio is indicated hereafter as Cu#). In particular, the lower this value, the higher is the As + Sb + Bi deficit with respect to the ideal value of 2 apfu (Fig. 3b). This seems to suggest a role of elements other than Cu in the replacement of As, Sb and Bi. This kind of replacement seems to affect all possible samples of watanabeite, disregarding the ratio As/(As+Sb+Bi) (hereafter As#). Indeed, the Cu# has no clear correlation with As# (Fig. 3c).

On the basis of these observations, the most likely mechanism favouring the incorporation of formally divalent metals in watanabeite may be the substitution $Cu^{+} + As^{3+} = 2\ Me^{2+}$, with the replacement possibly involving different Me^{2+} cations. Indeed, in the specimen studied from the Pefka ore deposit, ~0.25 Pb^{2+} apfu replaces ~0.25 $(As+Sb)^{3+}$ apfu. Such a substitution creates a charge imbalance, that could be neutralised replacing Cu^{+} with formally divalent elements, e.g. Fe^{2+} (0.10 apfu) and, possibly, of ~0.15 Cu^{2+}. The occurrence of Fe^{3+}, possibly involved in the substitution mechanism $Cu^{+} + 2\ (As,Sb)^{3+} = Fe^{3+} + 2\ Pb^{2+}$ is not supported by available data.

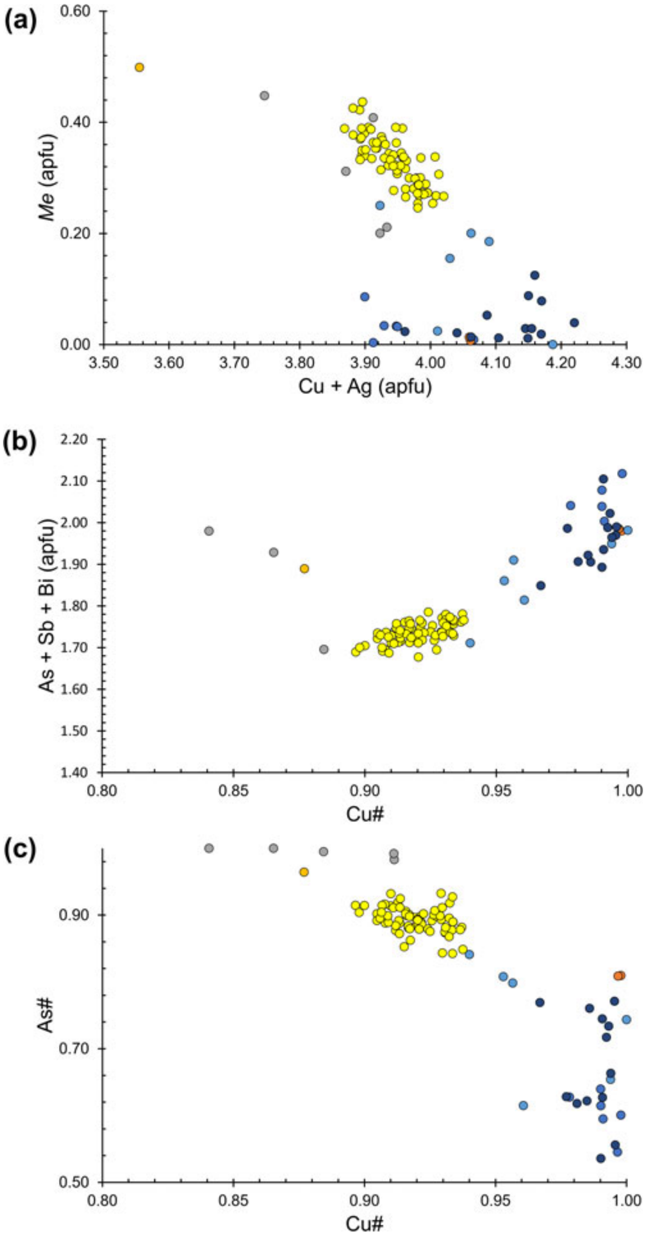

Figure 3. Chemical variability in watanabeite. Same symbols as in Fig. 2.

Crystal structure

The crystal structure of watanabeite (Fig. 4) shows six independent Cu sites, three As positions, one split and mixed (Sb,As/Pb)-hosting *M*(1) site, and eight S positions. In the following, the details of atom coordinations and site occupancies will be discussed before giving a general outline of the crystal structure of this copper sulfosalt.

Atom coordinations and site occupancies

Copper sites are characterised by tetrahedral and triangular coordination. Copper atoms hosted at the Cu(1), Cu(2) and Cu(3) sites are tetrahedrally coordinated, with <Cu–S> distances ranging between 2.308 and 2.323 Å. These distances can be compared with those reported for other tetrahedrally coordinated Cu sites, e.g. in the virtually pure Cu site *M*(1) of stibiogoldfieldite (2.329 Å – Biagioni *et al.*, 2022c) or in chalcopyrite-like minerals

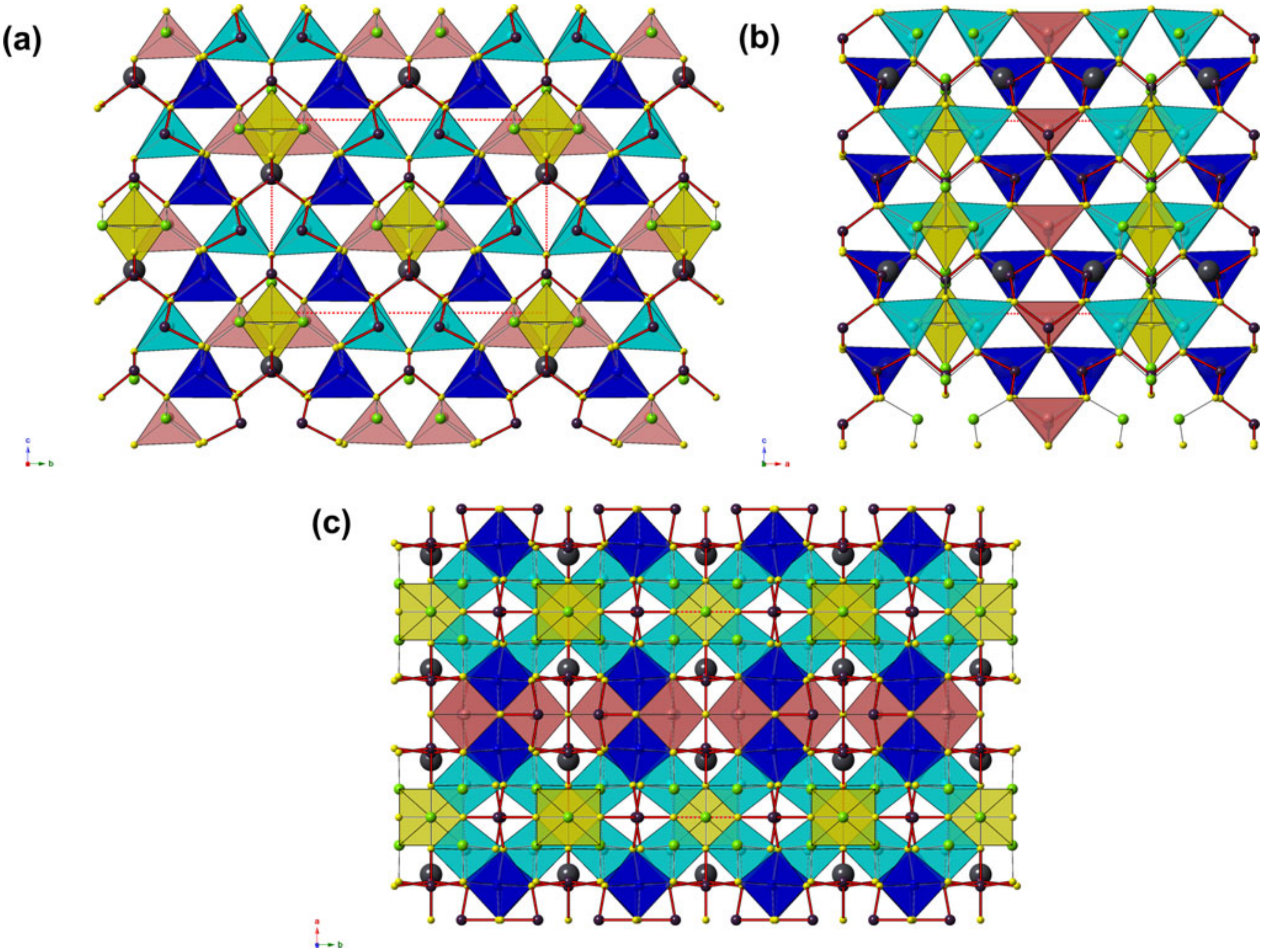

Figure 4. Crystal structure of watanabeite as seen down [100] (a), [010] (b), and [001] (c). Polyhedra: dark blue = Cu(1) site; light blue = Cu(2) site; pink = Cu(3) site; yellow = S(8) site. Circles: green = Cu(4)-Cu(6) sites; violet = As(1)-As(3) and *M*(1a) sites; dark grey = *M*(1b) site; yellow = S(1)-S(7) sites. Red dotted lines indicated the unit cell, drawings made using CrystalMaker® software.

(2.302–2.33 – Hall, 1975). Bond-valence sums for these Cu atoms vary between 1.14 and 1.19 valence units (vu), agreeing with the occurrence of Cu^+.

Sites Cu(4), Cu(5) and Cu(6) host triangularly coordinated Cu atoms, with <Cu–S> distances in the range 2.241–2.254 Å. These values are similar to those reported in other Cu sulfides, e.g. in stibiogoldfieldite (2.251 Å – Biagioni *et al*., 2022c), tennantite-(Cd) (2.230 Å – Biagioni *et al*., 2022a), tennantite-(Cu) (2.230 Å – Biagioni *et al*., 2022b), and tetrahedrite-(Hg) (2.262 Å – Biagioni *et al*., 2020b). Bond-valence sums agree with the occurrence of Cu^+, being in the interval 1.02–1.08 vu.

No evidence for the replacement of Cu by other atoms was observed in both tetrahedrally and triangularly coordinated positions. However, it should be kept in mind that the amount of Fe (0.10 apfu) and Ag (0.01 apfu) is low and could not be detected during the crystal structure refinement. Moreover, the atomic number Z of Fe is similar to that of Cu ($Z = 26$ and 29, respectively), making their distinction more difficult.

Arsenic is hosted at the three pure sites As(1), As(2) and As(3). These sites show the typical trigonal pyramidal coordination of As^{3+}, with <As–S> distances in the range 2.247–2.266 Å. The corresponding bond-valence sums, in the range 2.95–3.11 vu, agree with the occurrence of As^{3+}.

Finally, a fourth position, namely *M*(1), is actually split into two sub-positions, *M*(1a) and *M*(1b), with *M*(1a)–*M*(1b) = 0.450(9) Å. The *M*(1a) position displays a trigonal pyramidal coordination, with three *Me*–S distances in the range 2.38–2.42 Å; this arrangement is compatible with a mixed (Sb,As) position. The *M*(1b) site has three short distances, in the range 2.61–2.63 Å, similar to a trigonal pyramidal coordination, and three additional very long distances close to 3.8 Å, with an average distance of ~3.2 Å. The mean atomic numbers (MANs) refined at the *M*(1a) and *M*(1b) positions are 15.87 and 42.56 electrons, respectively, summing to a total MAN at *M*(1) of 58.43 electrons. It agrees with the occurrence of Pb at this split position, partially replacing As and Sb. On the basis of the refined MANs, the observed bond distances, and the electron microprobe data, the site occupancies $(Sb_{0.21}As_{0.15})_{\Sigma 0.36}$ and $(Pb_{0.47}Sb_{0.17})_{\Sigma 0.64}$ are proposed for the partially occupied *M* (1a) and *M*(1b) positions, respectively. The total site occupancy of the *M*(1) site would be $(Pb_{0.47}Sb_{0.38}As_{0.15})_{\Sigma 1.00}$, corresponding to a theoretical MAN of 62.87 electrons, slightly higher than the observed one. The sum of the bond-valence sums, calculated using these proposed occupancies, is 2.55 vu, in agreement with a mixed (Pb^{2+}/Sb^{3+} and As^{3+}) position.

Sulfur atoms are usually four- or six-fold coordinated. Sulfur hosted at the S(1)–S(7) positions displays a tetrahedral coordination, possibly increased to higher coordination numbers if very long $^{M(1b)}$(Pb,Sb)–S distances are taken into account (when this sub-site is occupied). Two different kinds of coordination environments are observed, i.e. S bonded to three Cu atoms and one As atom [S(1) to S(5) sites] or S bonded to two Cu atoms and atoms hosted at two *M*(1) sites, actually split into *M*(1a) and *M*(1b) positions [S(6) and S(7) sites]. The former has a bond-valence sum ranging between 1.95 and 2.02 vu, whereas the latter is overbonded, showing bond-valence sums of 2.28–2.29 vu. The overbonding is possibly related to uncertainty in the actual environment around the split position *M*(1). Sulfur hosted at S(8) is octahedrally coordinated by Cu atoms, in a configuration similar to that observed for the S(2) site in tetrahedrite-group minerals (e.g. Biagioni *et al.*, 2020a). Its bond-valence sum is 2.08 vu, in agreement with the occurrence of S^{2-}.

Crystal structure architecture

The tetrahedrally coordinated sites, namely Cu(1), Cu(2) and Cu(3), are corner-bonded to form a three-dimensional framework (Fig. 4) having composition $Cu_{20}S_{38}$ ($Z = 1$). Cavities within the tetrahedral scaffolding are occupied by two different kinds of atom clusters. The first one is represented by triangularly coordinated Cu atoms, octahedrally arranged around a central S atom, hosted at the S(8) site, with composition $Cu_{12}S_2$ ($Z = 1$). Arsenic atoms hosted at the As(1) and As(2) sites encircle this SCu_6 anion-centred polyhedron. This configuration is the same observed in tetrahedrite-group minerals (e.g. Biagioni *et al.*, 2020a). The second kind of cluster is an $As_2(Pb,Sb,As)_2S_7$ group, formed by the As(3) and *M*(1) sites, bonded to S atoms hosted at the S(2), S(6) and S(7) sites, shared with the tetrahedral framework.

The structural formula of watanabeite from Pefka can thus be written as $^{[IV]}Cu_{20}S_{38} + {}^{[III]}Cu_{12}As_8S_2 + As_4(Pb,Sb,As)_4 = {}^{[III]}Cu_{12}\,{}^{[IV]}Cu_{20}As_{12}(Pb,Sb,As)_4S_{40}$ ($Z = 1$), that is $^{[III]}Cu_3\,{}^{[IV]}Cu_5As_3(Pb,Sb,As)S_{10}$ ($Z = 4$), considering the three independent three-fold Cu sites and the three independent tetrahedrally coordinated Cu sites as aggregated positions. The role of the *M*(1) site has to be better understood by examining further samples of watanabeite. On the basis of $Z = 8$, as currently reported in the official IMA List of Mineral Names (Pasero, 2024), the formula becomes $Cu_4As_{1.5}(Pb,Sb,As)_{0.5}S_5$.

Comparison between watanabeite and tetrahedrite-group minerals

Shimizu *et al.* (1993) pointed out the similarity between watanabeite and tetrahedrite-group minerals, based on physical properties and powder XRD patterns. Following the solution of the crystal structure of watanabeite, it is now possible to compare the structural arrangement of these sulfosalts. Both minerals are characterised by a three-dimensional framework formed by Cu-centred tetrahedra and show the occurrence of S-centred octahedra encircled by AsS_3 trigonal pyramids.

The distribution of this latter structural feature in watanabeite and tetrahedrite-group minerals is shown in Fig. 5. In watanabeite this cluster alternates, along **a**, with an $As_2(Pb,Sb,As)_2S_7$ cluster, not occurring in tetrahedrite-group minerals. This gives rise to a different distribution of the Cu_6As_4S clusters between watanabeite and tetrahedrite-group minerals.

In Fig. 6 a projection of the crystal structure of watanabeite, as seen down **c**, is compared with the crystal structure of a tetrahedrite-group mineral as seen down **a**. One can recognise a common structural module with composition $Cu_{10}As_4S_{13}$ ($Z = 2$); in watanabeite, these tetrahedrite-like modules are connected along [100] through the occurrence of symmetry-related Cu(1) sites, giving the composition $Cu_{10}Cu_4As_4S_{13}$ ($Z = 2$). It is worth noting that in tetrahedrite-group minerals, the position corresponding to the Cu(1) site in watanabeite has to be considered only half, giving the composition $Cu_{10}Cu_2As_4S_{13}$ ($Z = 2$), corresponding to the composition of tennantite-(Cu). In the crystal structure of watanabeite, the interspace between tetrahedrite-like modules is occupied by an additional slab with composition $Cu_2As_4S_7$ ($Z = 2$), where Pb is neglected; the thickness of this slab is ∼4 Å. Thus, the crystal structure of this sulfosalt can be described as a one-to-one intergrowth of tetrahedrite-like slabs and additional, As-rich, slabs, i.e. $Cu_{14}As_4S_{13} + Cu_2As_4S_7 = Cu_{16}As_8S_{20}$ ($Z = 2$) $= Cu_4As_2S_5$ ($Z = 8$).

Following these structural relationships, the unit-cell parameters of watanabeite and tetrahedrite-group minerals are related according to these equations: $a_{Wa} = a_{Ttd} \times \sqrt{2}/2 + \sim 4$ Å; $b_{Wa} = b_{Tnt} \times \sqrt{2}$; and $c_{Wa} \approx c_{Tnt}$.

The similarities between watanabeite and tetrahedrite-group minerals could suggest some crystal-chemical implications. For instance, Ag could be hosted preferentially at the triangularly

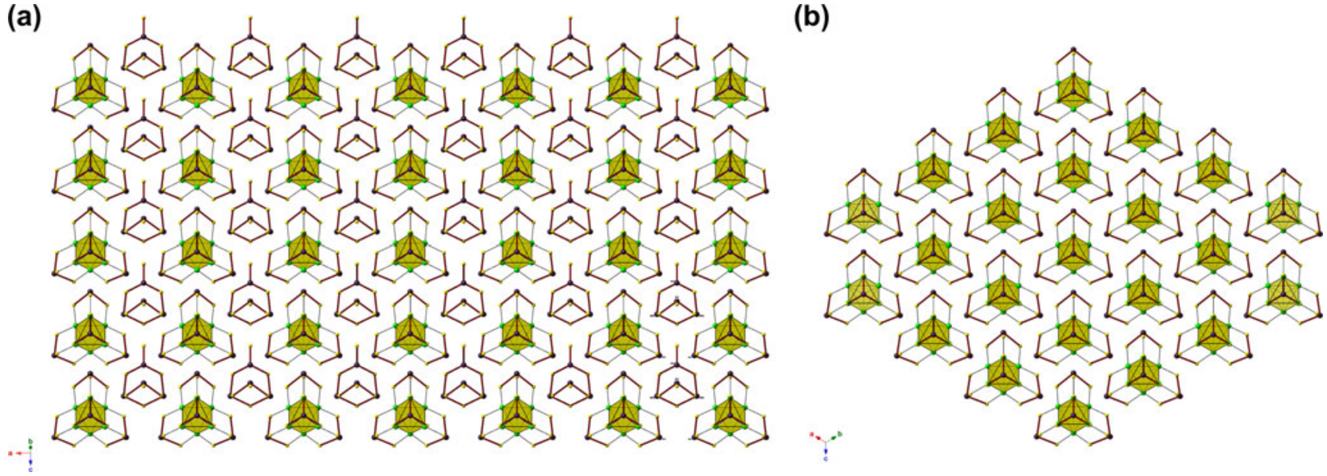

Figure 5. Comparison between the crystal structure of watanabeite, as seen down [011] (a) and tetrahedrite-group minerals, as seen down [111] (b).

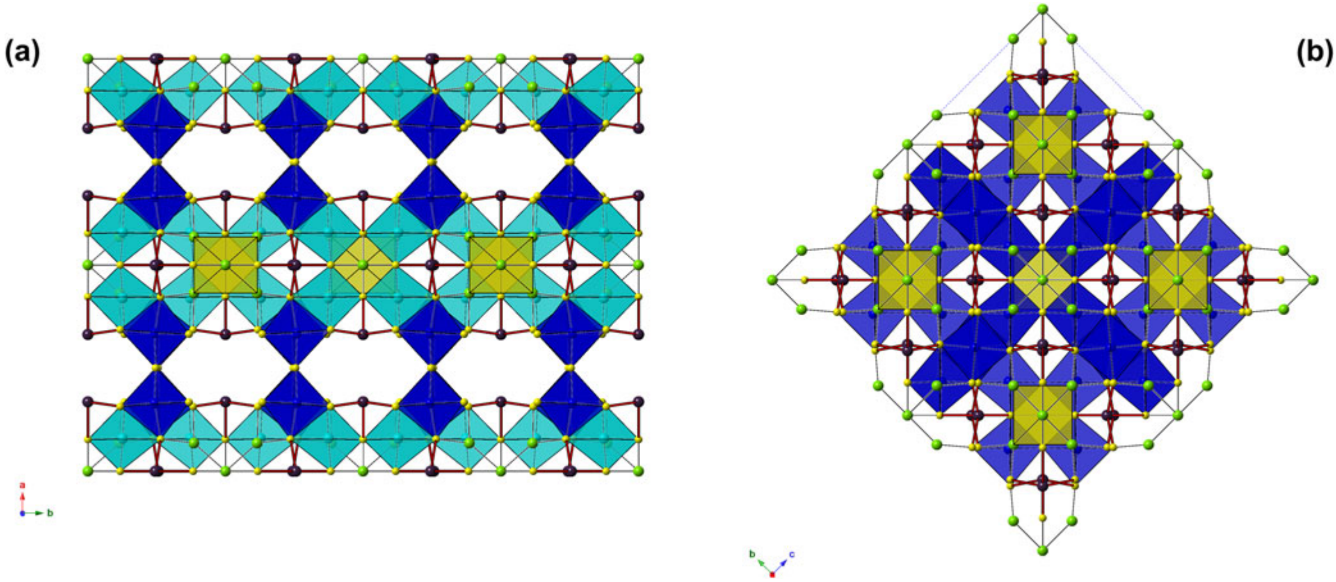

Figure 6. Comparison between the tetrahedrite-like slab of watanabeite, as seen down [001] (a) and the crystal structure of tetrahedrite-group minerals, as seen down [100] (b). Same symbols as in Figure 4.

coordinated Cu(4)–Cu(6) sites, as occurs in tetrahedrite-group minerals where Ag is preferentially located at the three-fold coordinated *M*(2) site (e.g. Kalbskopf, 1972). Moreover, the occurrence of the $Cu_6S(8)$ anion-centred polyhedra in the crystal structure of watanabeite may suggest that in Ag-rich environments and under peculiar physical–chemical conditions, some kinds of Ag–Ag interactions could occur, coupled with a S deficit, as observed in tetrahedrite-group minerals (e.g. Welch *et al.*, 2018; Biagioni *et al.*, 2020a). If Ag fully occupies the Cu(4)–Cu(6) sites, the ideal composition of the Ag-isotype would be $(Cu_{2.5}Ag_{1.5})_{\Sigma4.0}As_4S_5$ ($Z = 8$); the possible phase with vacancy dominant at the S(8) site and with the formation of metallic $(Ag_6)^{4+}$ clusters would have the chemical formula $(Cu_{2.5}Ag_{1.5})_{\Sigma4.0}As_4S_{4.75}\square_{0.25}$ ($Z = 8$). Currently, the highest Ag content reported in watanabeite is 0.22 Ag apfu from the St. Philippos deposit, Greece (Voudouris *et al.*, 2005), well below the value proposed for the Ag-isotype of watanabeite. Such a content could correspond to the full occupancy of Cu(5) or Cu(6) sites; however, a crystal structure study of Ag-bearing watanabeite is mandatory to ascertain the ordering of Ag.

Finally, the solution of the crystal structure of Pb-bearing watanabeite indicates a possible mechanism favouring the incorporation of a large-sized cation such as Pb^{2+} in a tetrahedrite-like tetrahedral framework. Indeed, the occurrence of Pb is reported in some samples of tetrahedrite-group minerals. For instance, Vavelidis and Melfos (1997) documented the occurrence of Pb in tetrahedrite from the Maronia area, Greece, with Pb dominating over Fe and Zn. However, Makovicky and Karup-Møller (1994) observed a maximum Pb content in synthetic samples of 0.45 apfu and they were not able to exclude the possible existence of very fine exsolution of Pb-rich phases within the tetrahedrite matrix. Moreover, it is possible that some occurrences of Pb-bearing tetrahedrite-group minerals are actually Pb-bearing watanabeite, considering the similarity in the physical properties and chemical formula, as discussed above. For instance, the average analysis of Pb-rich tetrahedrite from Maronia (Vavelidis and Melfos, 1997), i.e. $(Cu_{10.69}Ag_{0.04})_{\Sigma10.73}(Pb_{0.96}Fe_{0.19}Zn_{0.03})_{\Sigma1.18}(Sb_{4.02}As_{0.04})_{\Sigma4.06}S_{13.03}$, can be recalculated on the basis of 11 apfu, i.e. $(Cu_{4.05}Ag_{0.02})_{\Sigma4.07}(Pb_{0.36}Fe_{0.07}Zn_{0.01})_{\Sigma0.44}(Sb_{1.52}As_{0.02})_{\Sigma1.54}S_{4.94}$, with a Cu^*/As^* ratio of 2.18. This formula is similar to that of Pb-bearing watanabeite (even if Sb > As, and consequently the species would be an Sb-analogue), with a deficit of (Sb+As) similar to the sum of divalent elements (Pb, Fe, Zn). This suggests that further data are needed to ascertain the identity of Pb-rich tetrahedrite-group minerals that could be misidentified on the basis of chemical data only.

Watanabeite in the framework of Cu–As–S phases

Watanabeite belongs to the Cu–As–S ternary system, currently formed by six different mineral species (Table 6). Maske and Skinner (1971) investigated this system finding enargite, lautite, luzonite, sinnerite, 'tennantite', and a new compound ('compound A'), with formula $Cu_{24}As_{12}S_{31}$, i.e. $Cu_4As_2S_{5.167}$. Shimizu *et al.* (1993) compared the powder XRD pattern of watanabeite with that of 'compound A' of Maske and Skinner (1971), pointing out the similarity. Some similarities can also be found with the 'compound C' synthesised in the Cu–Sb–As–S system by Luce *et al.* (1977). This phase has composition $Cu_4(As/Sb)_2S_5$, with the As/(As+Sb) ratio ranging between 0.455 to 0.74, that is from Sb-dominant to As-dominant.

Watanabeite contains As^{3+}, as confirmed by the solution of its crystal structure. In this respect it is similar to sinnerite and tennantite-(Cu), both being As^{3+}-species (Bindi *et al.*, 2013; Biagioni *et al.*, 2022b). On the contrary, enargite and luzonite are two dimorphs of the compound Cu_3AsS_4, showing tetrahedrally coordinated As^{5+} cations (Marumo and Nowacki, 1967; Karanović *et al.*, 2002). More complex is the crystal structure of lautite, where As–As bonding was also observed (e.g. Bindi *et al.*, 2008).

The different oxidation state of As could be related to different f_{S_2} of the crystallisation medium, with the high value of f_{S_2} favouring the formation of As^{5+} compounds, whereas lower values may stabilise As^{3+}-phases, among which is watanabeite.

Table 6. Minerals belonging to the Cu–As–S ternary system.

Mineral	Chemical formula	*a* (Å)	*b* (Å)	*c* (Å)	α (°)	β (°)	γ (°)	s.g.	Reference
Enargite	Cu_3AsS_4	7.41	6.44	6.16	90	90	90	$Pmn2_1$	Karanović *et al.* (2002)
Lautite	CuAsS	11.35	3.75	5.45	90	90	90	*Pnma*	Bindi *et al.* (2008)
Luzonite	Cu_3AsS_4	5.33	5.33	10.57	90	90	90	$I\bar{4}2m$	Marumo and Nowacki (1967)
Sinnerite	$Cu_6As_4S_9$	9.10	9.86	9.11	90.3	109.6	107.6	*P*1	Bindi *et al.* (2013)
Tennantite-(Cu)	$Cu_{12}As_4S_{13}$	10.17	10.17	10.17	90	90	90	$I\bar{4}3m$	Biagioni *et al.* (2022b)
Watanabeite	$Cu_4As_2S_5$	10.96	14.65	10.30	90	90	90	*Amm*2	This work

s.g. = space group.

Conclusion

The solution of the crystal structure of watanabeite reveals a potentially more complex crystal chemistry than that suggested by the chemical formula $Cu_4As_2S_5$. Indeed, several substitutions are observed in natural samples, allowing the incorporation of other cations than Cu having different sizes, such as Pb, Fe and Zn. For this reason, the crystal chemical investigation of more samples, characterised by different chemistries, would be useful, allowing a better understanding of this sulfosalt that is able to host several elements typical of hydrothermal environments. A crystallographic investigation of samples with Sb > As is also mandatory, in order to understand the relationship between watanabeite and its chemically Sb-analogue. Finally, it is probable that several occurrences of watanabeite may have been misidentified, owing to its similarity with tetrahedrite-group minerals. Taking into account the progresses in mineralogical crystallography, allowing the full characterisation of very small grains (less than 50 μm in size), a complete characterisation of the mineralogy of ore deposits should consider the possibility of coupling electron microprobe analyses with XRD data. This would increase our understanding of the mineral systematics and the processes governing the ore formation.

Acknowledgements. The comments of the Associate Editor František Laufek and the revision by Luca Bindi, Peter Leverett, and an anonymous reviewer helped us in improving the paper. CB acknowledges financial support from the Ministero dell'Istruzione, dell'Università e della Ricerca through the project PRIN 2017 "TEOREM – deciphering geological processes using Terrestrial and Extraterrestrial ORE Minerals", prot. 2017AK8C32. JS and ZD acknowledge financial support from the Ministry of Culture of the Czech Republic (long-term project DKRVO 2024-2028/1.II.a; National Museum, 00023272). The Centro per l'Integrazione della Strumentazione scientifica dell'Università di Pisa (C.I.S.U.P.) is acknowledged for the access to the C.I.S.U.P. X-ray Laboratory.

Supplementary material. The supplementary material for this article can be found at https://doi.org/10.1180/mgm.2024.14.

Competing interests. The authors declare none.

References

Ahmed M., Shaif M., Siddiquie F.N. and Khan R. (2018) Mode of occurrence and mineralogy of northern Khetri copper deposits, Jhunjhunu district, Rajasthan. *Natural Resources*, **9**, 389–403.

Biagioni C., George L.L., Cook N.J., Makovicky E., Moëlo Y., Pasero M., Sejkora J., Stanley C.J., Welch M.D. and Bosi F. (2020a) The tetrahedrite group: Nomenclature and classification. *American Mineralogist*, **105**, 109–122.

Biagioni C., Sejkora J., Musetti S., Velebil D. and Pasero M. (2020b) Tetrahedrite-(Hg), a new 'old' member of the tetrahedrite group. *Mineralogical Magazine*, **84**, 584–592.

Biagioni C., Kasatkin A., Sejkora J., Nestola F. and Škoda R. (2022a) Tennantite-(Cd), $Cu_6(Cu_4Cd_2)As_4S_{13}$, from the Berenguela mining district, Bolivia: the first Cd-member of the tetrahedrite group. *Mineralogical Magazine*, **86**, 834–840.

Biagioni C., Sejkora J., Moëlo Y., Marcoux E., Mauro D. and Dolníček Z. (2022b) Tennantite-(Cu), $Cu_{12}As_4S_{13}$, from Layo, Arequipa Department, Peru: a new addition to the tetrahedrite-group minerals. *Mineralogical Magazine*, **86**, 331–339.

Biagioni C., Sejkora J., Musetti S., Makovicky E., Pagano R., Pasero M. and Dolníček Z. (2022c) Stibiogoldfieldite, $Cu_{12}(Sb_2Te_2)S_{13}$, a new tetrahedrite-group mineral. *Mineralogical Magazine*, **86**, 168–175.

Bindi L., Catelani T., Chelazzi L. and Bonazzi P. (2008) Reinvestigation of the crystal structure of lautite, CuAsS. *Acta Crystallographica*, **E64**, i22.

Bindi L., Makovicky E., Nestola F. and De Battisti L. (2013) Sinnerite, $Cu_6As_4S_9$, from the Lengenbach quarry, Binn Valley, Switzerland: description and re-investigation of the crystal structure. *The Canadian Mineralogist*, **51**, 851–860.

Brese N.E. and O'Keeffe M. (1991) Bond-valence parameters for solids. *Acta Crystallographica*, **B47**, 192–197.

Efremov S.V., Spiridonov A.M., Goryachev N.A. and Budyak A.E. (2021) Evolution of the Kara ore-magmatic system (Eastern Transbaikalia, Russia): experience in applying small-scale geochemical survey. *Geology of Ore Deposits*, **63**, 257–268.

Flack H.D. (1983) On enantiomorph-polarity estimation. *Acta Crystallographica*, **A39**, 876–881.

Hall S.R. (1975) Crystal structures of the chalcopyrite series. *The Canadian Mineralogist*, **40**, 699–710.

Kalbskopf R. (1972) Strukturverfeinerung des Freibergits. *Tschermaks Mineralogische und Petrographische Mitteilungen*, **18**, 147–155.

Karanović L., Cvetković L., Poleti D., Balić-Žunić T. and Makovicky E. (2002) Crystal and absolute structure of enargite from Bor (Serbia). *Neues Jahrbuch für Mineralogie, Monatshefte*, **2002**, 241–253.

Luce F.D., Tuttle C.L. and Skinner B.J. (1977) Studies of sulfosalts of copper: V. Phases and phase relations in the system Cu-Sb-As-S between 350° and 500°C. *Economic Geology*, **72**, 271–289.

Makovicky E. and Karup-Møller S. (1994) Exploratory studies on substitution of minor elements in synthetic tetrahedrite. Part I. Substitution by Fe, Zn, Co, Ni, Mn, Cr, V and Pb. Unit-cell parameter changes on substitution and the structural role of "Cu^{2+}". *Neues Jahrbuch für Mineralogie, Abhandlungen*, **167**, 89–123.

Makovicky E., Karanović L., Poleti D. and Balić-Žunić T. (2005) Crystal structure of copper-rich unsubstituted tennantite, $Cu_{12.5}As_4S_{13}$. *The Canadian Mineralogist*, **43**, 679–688.

Márquez-Zavalía M.F. and Galliski M.A. (2007) Chatkalita, nekrasovita y otros minerales del grupo de la estannita de Veta María Eugenia, Cerro Atajo, Catamarca. *Revista de la Asociación Geológica Argentina*, **62**, 289–298.

Marumo F. and Nowacki W. (1967) A refinement of the crystal structure of luzonite, Cu_3AsS_4. *Zeitschrift für Kristallographie*, **124**, 1–8.

Maske S. and Skinner B.J. (1971) Studies of the sulfosalts of copper. I. Phases and phase relations in the system Cu–As–S. *Economic Geology*, **66**, 901–918.

Paar W.H., Topa D. and Sureda R.J. (2002) Watanabeíta, $Cu_4(As,Bi,Sb)_2S_5$, con una nueva fase mineral "Cu_3AsS_3" en Cerro Atajo, provincia de Catamarca, Argentina. *Facultad de Ciencias Exactas y Naturales* (*UBA*) *Mineralogía y Metalogenia, Actas*, **2002**, 329–332.

Papavasiliou K., Voudouris P., Kanellopoulos C., Alfieris D. and Xydous S. (2016) Mineralogy and geochemistry of the Triades-Galana Pb-Zn-Ag-Au intermediate-high sulfidation epithermal mineralization, Milos Island, Greece. *Bulletin of the Geological Society of Greece*, **50**, 13 pp.

Pasero M. (2024) *The New IMA List of Minerals*. International Mineralogical Association. Commission on new minerals, nomenclature and classification (IMA-CNMNC). http://cnmnc.units.it/.

Pouchou J.L. and Pichoir F. (1985) “PAP” (φρZ) procedure for improved quantitative microanalysis. Pp. 104–106 in: *Microbeam Analysis* (J.T. Armstrong, editor). San Francisco Press, San Francisco.

Repstock A., Voudouris P. and Kolitsch U. (2015) New occurrences of watanabeite, colusite, “arsenosulvanite”, and “Cu-excess” tetrahedrite-tennantite at the Pefka high-sulfidation epithermal deposit, northeastern Greece. *Neues Jahrbuch für Mineralogie, Abhandlungen*, **192**, 135–149.

Sheldrick G.M. (2015) Crystal Structure Refinement with SHELXL. *Acta Crystallographica*, **C71**, 3–8.

Shimizu M., Kato A., Matsubara S., Criddle A.J. and Stanley C.J. (1993) Watanabeite, $Cu_4(As,Sb)_2S_5$, a new mineral from the Teine mine, Sapporo, Hokkaido, Japan. *Mineralogical Magazine*, **57**, 643–649.

Sidorov E.G., Borovikov A.A., Tolstykh N.D., Bukhanova D.S., Palyanova G.A. and Chubarov V.M. (2020) Gold mineralization at the Maletoyvayam deposit (Koryak Highland, Russia) and physicochemical conditions of its formation. *Minerals*, **10**, 1093.

Vavelidis M. and Melfos V. (1997) Two plumbian tetrahedrite-tennantite occurrences from Maronia area (Thrace) and Milos island (Aegean sea), Greece. *European Journal of Mineralogy*, **9**, 653–658.

Voudouris P., Papavasiliou C. and Melfos V. (2005) Silver mineralogy of St. Philippos deposit (NE Greece) and its relationship to a Te-bearing porphyry-Cu-Mo mineralization. *Geochemistry, Mineralogy and Petrology*, **43**, 155–160.

Voudouris P.C., Melfos V., Spry P.G., Moritz R., Papavassiliou C. and Falalakis G. (2011) Mineralogy and geochemical environment of formation of the Perama Hill high-sulfidation epithermal Ag-Ag-Te-Se deposit, Petrota Graben, NE Greece. *Mineralogy and Petrology*, **103**, 79–100.

Voudouris P., Biagioni C., Sejkora J. and Musetti S. (2023) Tennantite-(In), IMA 2023-011. In: CNMNC Newsletter, 73. *European Journal of Mineralogy*, **35**, 397–402.

Warr L.N. (2021) IMA–CNMNC approved mineral symbols. *Mineralogical Magazine*, **85**, 291–320.

Welch M.D., Stanley C.J., Spratt J. and Mills S.J. (2018) Rozhdestvenskayaite $Ag_{10}Zn_2Sb_4S_{13}$ and argentotetrahedrite $Ag_6Cu_4(Fe^{2+},Zn)_2Sb_4S_{13}$: two Ag-dominant members of the tetrahedrite group. *European Journal of Mineralogy*, **30**, 1163–1172.

Wilson A.J.C. (1992) *International Tables for Crystallography. Volume C*. Kluwer, Dordrecht, The Netherlands.

Zheng S.J., Zhong H., Bai Z.J, Zhang Z.K. and Wu C.Q. (2021) High-sulfidation veins in the Jiama porphyry system, South Tibet. *Mineralium Deposita*, **56**, 205–214.